Structural Engineering and Mechanics, Vol. 21, No. 5 (2005) 571-590
DOI: http://dx.doi.org/10.12989/sem.2005.21.5.571

A hybrid 8-node hexahedral element for static and free vibration analysis

Kutlu Darılmaz†

Department of Civil Engineering, Istanbul Technical University 34469, Maslak, Istanbul, Turkey

(Received April 27, 2005, Accepted September 5, 2005)

Abstract. An 8 node assumed stress hexahedral element with rotational degrees of freedom is proposed for static and free vibration analyses. The element formulation is based directly on an 8-node element. This direct formulation requires fewer computations than a similar element that is derived from an internal 20-node element in which the midside degrees of freedom are eliminated by expressing them in terms of displacements and rotations at corner nodes. The formulation is based on Hellinger-Reissner variational principle. Numerical examples are presented to show the validity and efficiency of the present element for static and free vibration analysis.

Key words: solid element; 8-node hexahedral element; hybrid finite element; static analysis; free vibration.

1. Introduction

The 8-node hexahedral element is widely used in the analysis of 3D elasticity problems for its outstanding merits, such as simplicity, easy application and high accuracy. This element can be easily found in most of element libraries of structural analysis programs and the modeling of complicated 3D structures by this element is relatively easier than other solid elements. Therefore, a great deal of attention has been paid to develop an efficient hexahedral element. Continous research efforts have been devoted in the recent years to the development of the more efficient and accurate hexahedral elements. Chandra and Prathap (1989) presented an 8-noded solid element by using field consistent formulation; Chen and Cheung (1992) presented two elements with independent variables of strain, stress and displacement and with a weaker constraint condition of interelement continuity; Sze and Ghali (1993) proposed a robust two-field hexahedral element capable of handling plate/shell, beam and nearly incompressible material analyses; Yeo and Lee (1997) presented a new stress assumption for hybrid stress elements and adapted to the eight-node hybrid stress brick element; Rajendran and Prathap (1999) proposed a field consistent eight-node hexahedron element and investigated its performance in free vibration analysis; Sze and Yao (2000) proposed an eight-node solid-shell element based on the assumed natural strain method, Cao *et al.* (2002) presented a penalty-equilibrating 3D-mixed element based on the Hu-Washizu variational principle; Chen and Wu (2004) proposed a mixed 8-node hexahedral element based on the Hu-Washizu principle and

† Research Assistant (Ph.D.), E-mail: kdarilmaz@ins.itu.edu.tr

the field extrapolation technique.

One of the methods to improve the element performance is developing the element with rotational degrees of freedom. This method avoids the use of higher order elements which have mid-edge nodes and provides an easy coupling with other type of elements such as beams and shells which have rotational degree of freedom. Various solid elements have been developed with rotational degrees of freedom. Yunus *et al.* (1991) introduced an 8-node solid hexahedron element having corner rotations which are introduced by transformation of the midside translational degree of freedom of a 20-node hexahedron element; Ibrahimbegovic and Wilson (1991) presented thick shell and solid elements which are derived from variational principles employing independent rotation fields; Choi and Chung (1996) proposed an 8-node solid element having corner rotations which are introduced by transforming the hierarchical mid-edge displacements with parabolic shape along an edge; Sze *et al.* (1996) proposed two solid elements equipped with Allman's rotation and Choi *et al.* (2001) presented a three-dimensional 13-node hexahedral element which is established by adding five nodes to one of the six faces of basic 8-node hexahedral element.

Since the pioneering work of Pian (1964) for hybrid stress elements, great efforts have been devoted to develop high-performance stress assumptions. The main issues have been coordinate invariance, satisfaction of equilibrium conditions and sensitivity to mesh distortion. In the early stage of development, hybrid stress elements are based on the principle of minimum complementary energy and assumed stresses need to be defined in a Cartesian coordinate system for pointwise satisfaction of the equilibrium conditions. Although this approach is rational, the performance of the resulting assumed stress elements are affected very much by mesh distortion and it is not easy to satisfy coordinate invariance and equilibrium conditions simultaneously. To overcome these weaknesses, Pian and Sumihara (1984) proposed a new approach for hybrid stress elements that is based on the Hellinger-Reissner principle and defined the assumed stresses in the natural coordinate system.

The present paper develops an 8-node assumed stress hybrid hexahedral element including translations and rotations as nodal d.o.f. The formulation is based directly on 8-node element from the beginning in contrast to elements whose formulations began with an internal 20-node element. Formulating the element in this manner bypasses the formation of the stiffness matrix for an 20-node element and the subsequent transformation of this stiffness matrix to that corresponding to the stiffness matrix of an 8-node element. This method is advantageous in that the element formulation is more direct and savings in computations are accrued. Results are presented for static and free vibration analysis to show the validity and efficiency of the present element.

2. Element stiffness formulation

The assumed-stress hybrid method is based on the independent prescriptions of stresses within the element and displacements on the element boundary. The element stiffness matrix is obtained using Hellinger-Reissner variational principle. The Hellinger-Reissner functional of linear elasticity allows displacements and stresses to be varied separately. This establishes the master fields. Two slave strain fields appear, one coming from displacements and one from stresses.

The Hellinger-Reissner functional can be written as

$$\Pi_{RH} = \int_V \{\sigma\}^T [D]\{u\} dV - \frac{1}{2}\int_V \{\sigma\}^T [S]\{\sigma\} dV \tag{1}$$

where $\{\sigma\}$ is the vector of assumed stresses, $[S]$ is the material compliance matrix relating strains, $\{\varepsilon\}$, to stress ($\{\varepsilon\} = [S]\{\sigma\}$), $[D]$ is the differential operator matrix corresponding to the linear strain-displacement relations ($\{\varepsilon\} = [D]\{u\}$) and V is the volume of structure. In Eq. (1), the load potential is omitted as it is not required for formulating the element stiffness matrix.

The assumed stress field is described in the interior of the element as

$$\{\sigma\} = [P]\{\beta\} \tag{2}$$

and a compatible displacement field is described by

$$\{u\} = [N]\{q\} \tag{3}$$

where $[P]$ and $[N]$ are matrices of stress and displacement interpolation functions, respectively, and $\{\beta\}$ and $\{q\}$ are the unknown stress and nodal displacement parameters, respectively. Intra-element assumed stresses and compatible displacements are independently interpolated. Since stresses are independent from element to element, the stress parameters are eliminated at the element level and a conventional stiffness matrix results. This leaves only the nodal displacement parameters to be assembled into the global system of equations.

Substituting the stress and displacement approximations Eq. (2), Eq. (3) in the functional Eq.(1)

$$\Pi_{RH} = [\beta]^T[G][q] - \frac{1}{2}[\beta]^T[H][\beta] \tag{4}$$

where

$$[H] = \int_V [P]^T[S][P]dV \tag{5}$$

$$[G] = \int [P]^T([D][N])dV \tag{6}$$

Now imposing stationary conditions on the functional with respect to the stress parameters, $\{\beta\}$ gives

$$[\beta] = [H]^{-1}[G][q] \tag{7}$$

Substitution of $\{\beta\}$ in Eq. (4), the functional reduces to

$$\Pi_{RH} = \frac{1}{2}[q]^T[G]^T[H]^{-1}[G][q] = \frac{1}{2}[q]^T[K][q] \tag{8}$$

where

$$[K] = [G]^T[H]^{-1}[G] \tag{9}$$

is recognized as a stiffness matrix.

The solution of the system yields the unknown nodal displacements $\{q\}$. After $\{q\}$ is determined, element stresses or internal forces can be recovered by the use of Eq. (7) and Eq. (2). Thus

$$\{\sigma\} = [P][H]^{-1}[G]\{q\} \tag{10}$$

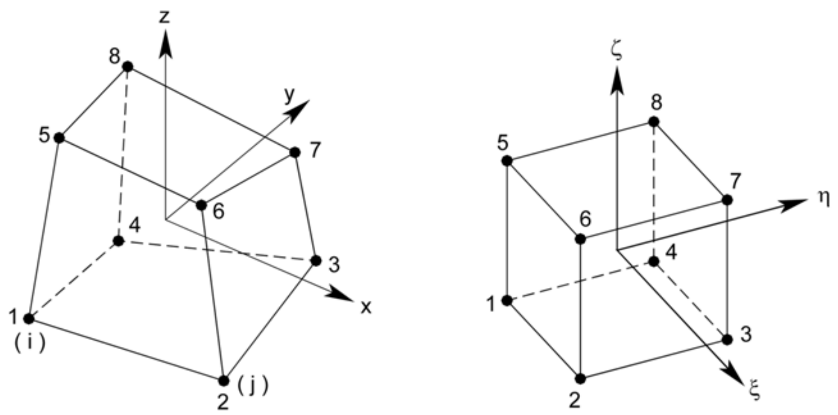

Fig. 1 HBHEX8R element

The displacement field of the element is defined by treating the edges as beam elements with shear deformation. Formulation of rotational d.o.f for the present element is based on the procedure given by Yunus *et al.* (1991) for their displacement based hexahedron and tetrahedron elements. For the typical edge *i-j* shown in Fig. 1 the displacements can be expressed as

$$\begin{aligned} u &= \frac{1}{2}[(1-\xi)u_i + (1+\xi)u_j] - \frac{z_j - z_i}{8}(1-\xi^2)(\theta_{yj} - \theta_{yi}) + \frac{y_j - y_i}{8}(1-\xi^2)(\theta_{zj} - \theta_{zi}) \\ v &= \frac{1}{2}[(1-\xi)v_i + (1+\xi)v_j] + \frac{z_j - z_i}{8}(1-\xi^2)(\theta_{xj} - \theta_{xi}) - \frac{x_j - x_i}{8}(1-\xi^2)(\theta_{zj} - \theta_{zi}) \\ w &= \frac{1}{2}[(1-\xi)w_i + (1+\xi)w_j] + \frac{x_j - x_i}{8}(1-\xi^2)(\theta_{yj} - \theta_{yi}) - \frac{y_j - y_i}{8}(1-\xi^2)(\theta_{xj} - \theta_{xi}) \end{aligned} \tag{11}$$

where $(x_i\ y_i\ z_i)$ and $(x_j\ y_j\ z_j)$ are the coordinates of joints i and j respectively with respect to the reference local element xyz coordinate system. Eq. (11), when extended to all sides of the element, indicates that 24 rotational d.o.f. in addition to the usual 24 displacement d.o.f. are required to express the displacements as quadratic functions. As opposed to conventional 8-node solid elements which have 24 degrees of freedom, elements with rotational degrees of freedom have 48 degrees of freedom.

The biggest difficulty in deriving hybrid finite elements seems to be the lack of a rational methodology for deriving stress terms, Feng *et al.* (1997). It is recognized that the number of stress modes m in the assumed stress field should satisfy

$$m \geq n - r - p \tag{12}$$

with n the total number of nodal displacements, r the number of rigid body modes and p the number of zero-energy modes in an element. If Eq. (12) is not satisfied, the use of too few coefficients in $\{\beta\}$, the rank of the element stiffness matrix will be less than the total degrees of deformation freedom and the numerical solution of the finite element model will not be stable and produce an element with one or more mechanisms.

Increasing the number of β's by adding stress modes of higher-order term, each extra term will add more stiffness and stiffen the element, Pian and Chen (1983), Punch and Atluri (1984).

In determining the stress field, each of the stress components was represented by seven independent parameters. A complete linear stress field was first chosen for each stress component and for the quadratic terms, the higher order terms containing the coordinate direction in which the stress component acts were suppressed. This type of selection was found to yield better results from numerical experiments, Yunus *et al.* (1989). For the element under consideration n = 48, the number of rigid-body modes = 6, the number of zero-energy rotation modes = 6. Thus, the number of deformation modes = 48 – 6 – 6 = 36. To suppress the deformation modes, the minimum number of stress modes is 36. From numerical experimentations the author achieved that the following 42 parameter selection of stress field is somewhat more accurate and less sensitive to geometric distortion than fewer parameter selections.

Different type of stress selections can be found in Chen and Cheung (1992), Sze *et al.* (1996), Sze and Pan (2000).

The assumed stress field in the natural coordinates is given as

$$\begin{aligned}
\sigma_{\xi} &= \beta_1 + \beta_2\xi + \beta_3\eta + \beta_4\zeta + \beta_5\eta^2 + \beta_6\zeta^2 + \beta_7\eta\zeta \\
\sigma_{\eta} &= \beta_8 + \beta_9\xi + \beta_{10}\eta + \beta_{11}\zeta + \beta_{12}\xi^2 + \beta_{13}\zeta^2 + \beta_{14}\xi\zeta \\
\sigma_{\zeta} &= \beta_{15} + \beta_{16}\xi + \beta_{17}\eta + \beta_{18}\zeta + \beta_{19}\xi^2 + \beta_{20}\eta^2 + \beta_{21}\xi\eta \\
\tau_{\xi\eta} &= \beta_{22} + \beta_{23}\xi + \beta_{24}\eta + \beta_{25}\zeta + \beta_{26}\zeta^2 + \beta_{27}\xi\zeta + \beta_{28}\eta\zeta \\
\tau_{\eta\zeta} &= \beta_{29} + \beta_{30}\xi + \beta_{31}\eta + \beta_{32}\zeta + \beta_{33}\xi^2 + \beta_{34}\xi\eta + \beta_{35}\xi\zeta \\
\tau_{\zeta\xi} &= \beta_{36} + \beta_{37}\xi + \beta_{38}\eta + \beta_{39}\zeta + \beta_{40}\eta^2 + \beta_{41}\xi\eta + \beta_{42}\eta\zeta
\end{aligned} \tag{13}$$

Symbolically

$$\{\tilde{\sigma}\} = \{\sigma_{\xi}\ \ \sigma_{\eta}\ \ \sigma_{\zeta}\ \ \tau_{\xi\eta}\ \ \tau_{\eta\zeta}\ \ \tau_{\zeta\xi}\}^T \tag{14}$$

The stress field assumed in natural space is transformed to the global system using a natural to global tensor transformation matrix

$$\{\sigma\} = [T]\{\tilde{\sigma}\} \tag{15}$$

where $[T]$ is the transformation matrix at the element origin and can be expressed as

$$[T] = \begin{bmatrix}
J_{11}^2 & J_{21}^2 & J_{31}^2 & 2J_{11}J_{21} & 2J_{21}J_{31} & 2J_{31}J_{11} \\
J_{12}^2 & J_{22}^2 & J_{32}^2 & 2J_{12}J_{22} & 2J_{22}J_{32} & 2J_{32}J_{12} \\
J_{13}^2 & J_{23}^2 & J_{33}^2 & 2J_{13}J_{23} & 2J_{23}J_{33} & 2J_{33}J_{13} \\
J_{11}J_{12} & J_{21}J_{22} & J_{31}J_{32} & J_{11}J_{22}+J_{21}J_{12} & J_{21}J_{32}+J_{31}J_{22} & J_{31}J_{12}+J_{11}J_{32} \\
J_{12}J_{13} & J_{22}J_{23} & J_{32}J_{33} & J_{12}J_{23}+J_{22}J_{13} & J_{22}J_{33}+J_{32}J_{23} & J_{32}J_{13}+J_{12}J_{33} \\
J_{11}J_{13} & J_{21}J_{23} & J_{31}J_{33} & J_{11}J_{23}+J_{21}J_{13} & J_{21}J_{33}+J_{31}J_{23} & J_{31}J_{13}+J_{11}J_{33}
\end{bmatrix} \tag{16}$$

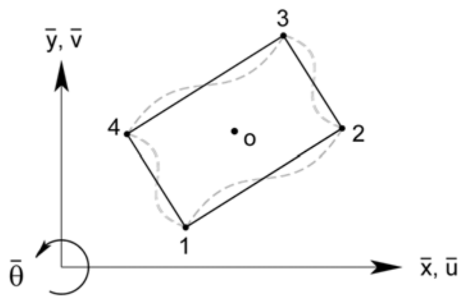

Fig. 2 Equal rotation and zero translation mode

$$[J_{ij}] = \left.\begin{bmatrix} \partial x/\partial\xi & \partial y/\partial\xi & \partial z/\partial\xi \\ \partial x/\partial\eta & \partial y/\partial\eta & \partial z/\partial\eta \\ \partial x/\partial\zeta & \partial y/\partial\zeta & \partial z/\partial\zeta \end{bmatrix}\right|_{\xi=\eta=\zeta=0} \tag{17}$$

J_{ij} terms are the components of the Jacobian matrix evaluated at the element origin.

The element stiffness matrix with rotational degrees of freedom exhibits equal-rotation mechanisms. These mechanisms were suppressed by artificially adding a small energy penalty to the stiffness matrix to make the stiffness matrix non-singular by generalizing the two dimensional stabilization schemes of MacNeal and Harder (1988). This method was also used by Yunus *et al.* (1991) for their displacement based hexahedron and tetrahedron elements.

Consider any face of the element and assume that the face lies in a local $\bar{x}-\bar{y}$ plane, Fig. 2. A relative rotation $\bar{\theta}_r$ is defined to be the difference between the average of the out of plane nodal rotation $\bar{\theta}$ and the average rotation $\bar{\theta}_o$ determined directly from the element shape functions as

$$\bar{\theta}_r = \frac{1}{\bar{n}}\sum_{i=1}^{\bar{n}}\bar{\theta}_i - \bar{\theta}_o \tag{18}$$

where $\bar{n}$, $\bar{\theta}_i$ are the numbers of nodes for the face and out of plane rotation at any node i, respectively.

$\bar{\theta}_o$ is the rotation at the element center and can be defined as

$$\bar{\theta}_o = \frac{1}{2}\left(\frac{\partial\bar{v}}{\partial\bar{x}} - \frac{\partial\bar{u}}{\partial\bar{y}}\right) \tag{19}$$

In terms of face system nodal degrees of freedom $\bar{u}_i$, $\bar{v}_i$, $\bar{\theta}_i$

$$\bar{\theta}_i = [\Phi]\{\bar{q}\} \tag{20}$$

where $\{\bar{q}\}$, $\{\Phi\}$ are face system nodal unknowns and relative rotation in terms of face system unknowns, respectively.

The energy penalty Λ is

$$\Lambda = \gamma VG[\bar{q}]\{\Phi\}[\Phi]\{q\} \tag{21}$$

Here γ is a dimensionless constant ($\gamma = 10^{-6}$ is recommended), V is the element volume and G is the shear modulus.

The vector of local face system unknowns $\{\bar{q}\}$ is related to global element degrees of freedom by

$$\begin{Bmatrix} \bar{u}_i \\ \bar{v}_i \\ \bar{\theta}_i \end{Bmatrix} = \begin{bmatrix} l_1 & m_1 & n_1 & 0 & 0 & 0 \\ l_2 & m_2 & n_2 & 0 & 0 & 0 \\ & & & l_3 & m_3 & n_3 \end{bmatrix} \begin{Bmatrix} u_i \\ v_i \\ w_i \\ \theta_{xi} \\ \theta_{yi} \\ \theta_{zi} \end{Bmatrix} \tag{22}$$

where l_i, m_i and n_i are direction cosines of the local face system.

Symbolically Eq. (22) is written as

$$\{\bar{q}\} = [\psi]\{q\} \tag{23}$$

The relationship for all face unknowns $\{\bar{q}\}$ with the related global unknowns $\{q\}$ can be written as

$$\{\bar{q}\} = \begin{bmatrix} [\Psi] & & & \\ & [\Psi] & & \\ & & [\Psi] & \\ & & & [\Psi] \end{bmatrix} \{q\} = [\Omega]\{q\} \tag{24}$$

Eq. (21) and Eq. (24) can be combined

$$\Lambda = [q](\gamma VG[\Omega]^T\{\Phi\}[\Phi][\Omega])\{q\} = [q][K_r]\{q\} \tag{25}$$

where

$$[K_r] = (\gamma VG)[\Omega]^T\{\Phi\}[\Phi][\Omega] \tag{26}$$

The penalty stiffness $[K_r]$ is added to the existing element stiffness matrix $[K]$ and the resulting stiffnes matrix is free from spurious equal rotation and zero translational modes.

3. Element mass matrix

The problem of determination of the natural frequencies of vibration reduces to the solution of the standard eigenvalue problem $[K] - \omega^2[M] = 0$, where ω is the natural angular frequency of the system. Making use of the conventional assemblage technique of the finite element method with the necessary boundary conditions, the system matrix $[K]$ and the mass matrix $[M]$ for the entire structure can be obtained.

Element mass matrix is derived from the kinetic energy expression

$$E_k = \frac{1}{2}\int_A \{\dot{q}\}^T [R]\{\dot{q}\} dA \tag{27}$$

where $\{\dot{q}\}$ denotes the velocity components and $[R]$ is the inertia matrix.

The nodal and generalized velocity vectors are related with the help of shape functions

$$\{\dot{q}\} = \sum_{i=1}^{8} [N]\{\dot{q}_i\} \tag{28}$$

Substituting the velocity vectors in the kinetic energy, Eq. (18) yields the mass matrix of an element.

$$E_k = \frac{1}{2}\int_A \{\dot{q}_i\}^T [N]^T [R][N]\{\dot{q}_i\} dA \tag{29}$$

$$E_k = \frac{1}{2}\int_A \{\dot{q}_i\}^T [m]\{\dot{q}_i\} dA \tag{30}$$

where $[m]$ is the element consistent mass matrix and is given by

$$[m] = \int_A [N]^T [R][N] dA \tag{31}$$

4. Numerical examples

Some standard numerical examples have been used for assessing the accuracy of the HBHEX8R element. The results obtained are compared with theoretical and some other element solutions that are available in open literature.

4.1 Example 1: Absence of spurious modes: examination of the stiffness matrix rank

The eigenvalues of the stiffness matrix $[K]$ for one element are computed for various shapes of the element. Six zero eigenvalues corresponding to the six rigid body motions of a solid are always obtained, showing thus a proper rank for the matrix $[K]$ and the absence of spurious modes in consequence.

4.2 Example 2: Patch test

The patch test proposed by MacNeal and Harder (1985) is used as a basic verification of the present element. The mesh configuration shown in Fig. 3 is used for constant stress states including σ_x, σ_y, σ_z, τ_{xy}, τ_{yz}, and τ_{xz}. The element passed the patch test.

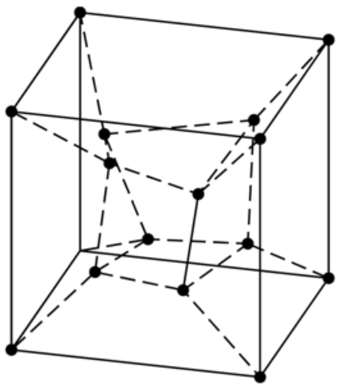

Fig. 3 Mesh for constant-stress test

4.3 Example 3: Cantilever beam

To evaluate the performance of the proposed element, a cantilever beam under a pure bending is investigated under two different meshes.

The vertical displacement and the rotation about *y*-axis at point A are presented respectively in Tables 1 and 2 with the theoretical solution for comparison (Timoshenko and Goodier 1951).

Stresses σ_x at point B are also listed in Table 3. It is also shown that the nonconforming elements and elements with rotational d.o.f give much improved results over the conventional conforming variable node element (C-V2).

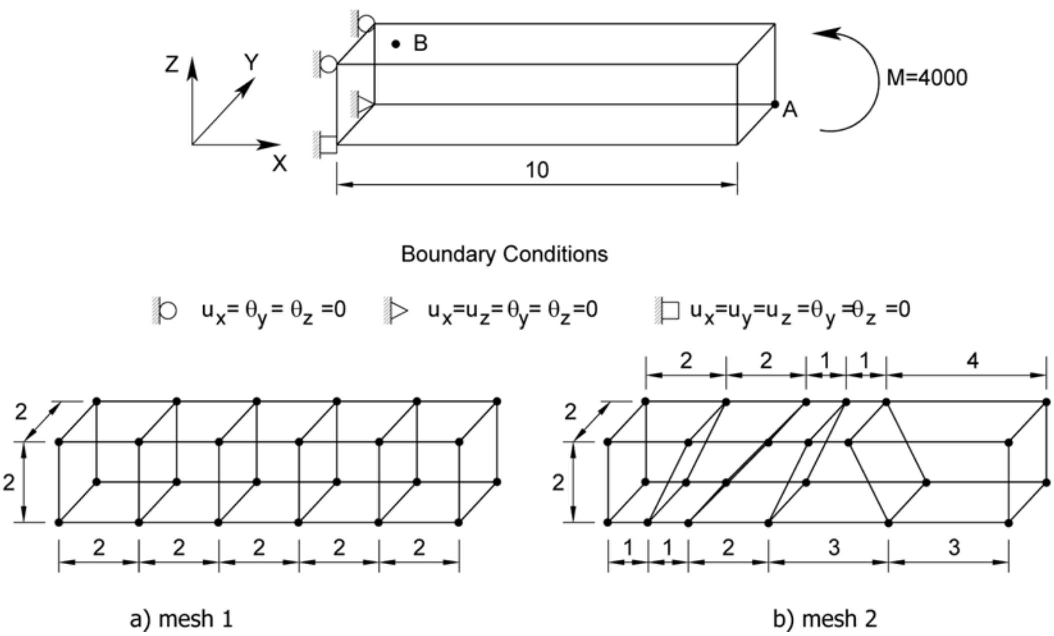

Fig. 4 Geometry, boundary conditions and mesh configuration of cantilever beam

Table 1 Vertical displacement of cantilever beam at point A

	Mesh 1	Mesh 2
C-V2 (Choi and Lee 1993)	66.67	44.38
NC-V1 (Choi and Lee 1993)	100.00	87.45
NCH-3 (Choi and Chung 1996)	100.00	97.33
MR-H8 (Choi *et al.* 2001)	93.75	81.09
HBHEX8R (This study)	96.12	83.47
Theory	100	100

Table 2 Rotation of cantilever beam at point A

	Mesh 1	Mesh 2
MR-H8 (Choi *et al.* 2001)	–18.75	–16.77
NCH-3 (Choi and Chung 1996)	–20.00	–18.62
HBHEX8R (This study)	–18.59	–16.32
Theory	–20	–20

Table 3 σ_x Stresses of cantilever beam at point B

	Mesh 1	Mesh 2
C-V2 (Choi and Lee 1993)*	–2200	–1736
NC-V1 (Choi and Lee 1993)**	–3000	–2262
NCH-3 (Choi and Chung 1996)**	–3000	–2270
MR-H8 (Choi *et al.* 2001)***	–3000	–2405
HBHEX8R (This study)***	–3000	–2613
Theoretical	–3000	–3000

*Conforming element without rotational d.o.f
**Non-Conforming element without rotational d.o.f
***Elements with rotational d.o.f

Results showed that the behaviour of the present element is satisfactory and results are in a good agreement with other solutions. When the distorted meshes are used the accuracy of stress solution obtained by HBHEX8R is superior to the accuracies obtained by other elements.

4.4 Example 4: Curved beam

A curved beam under in-plane and out of plane unit load is used for comparison. The dimensions and load are shown in Fig. 5, in which six elements are employed. The material constants are $E = 1.0 \times 10^7$ and $\nu = 0.3$ and the thickness of the beam is $t = 0.1$. In Table 4, the tip deflections obtained by other researchers and theoretical solution are used for comparison.

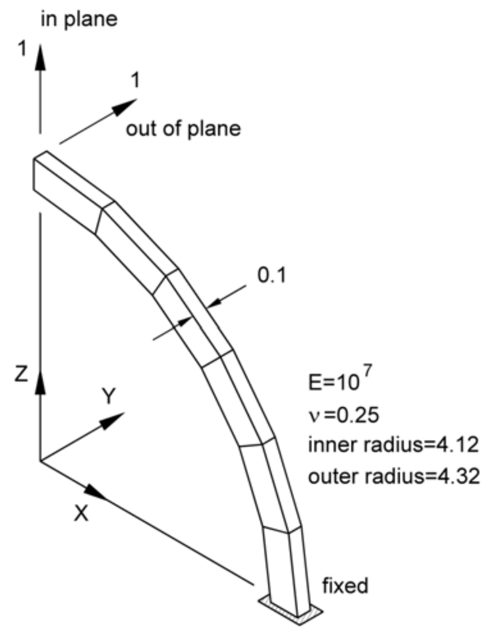

Fig. 5 Curved beam

Table 4 Tip deflections of the curved beam

	In plane	Out of plane
Yunus *et al*. (1991)	0.08708	0.4470
Sze and Ghali (1993)	0.07660	0.4249
Sze *et al.* (1996)	0.08707	0.4470
Sze and Lo (1999)	0.08933	0.4773
Sze and Pan (2000)	0.01782	0.3179
Cao *et al*. (2002)	0.08550	---
Chen and Wu (2004)	0.08848	0.4731
HBHEX8R (This study)	0.08752	0.4803
Theoretical	0.08734	0.5022

The theoretical value is extracted from Mac-Neal and Harder (1985). From this table, it can be found that the present element can predict better results compared with other elements.

4.5 Example 5: Simply supported square plate

This problem is depicted in Fig. 6. The plate is subjected to an uniform distributed loading. Owing to symmetry, a quarter of the plate is solved. Central deflections are normalized with given series solution cited in Ibrahimbegovic and Wilson (1991), see Table 5.

Results showed that the behaviour of the present element is satisfactory and converges to the reference value.

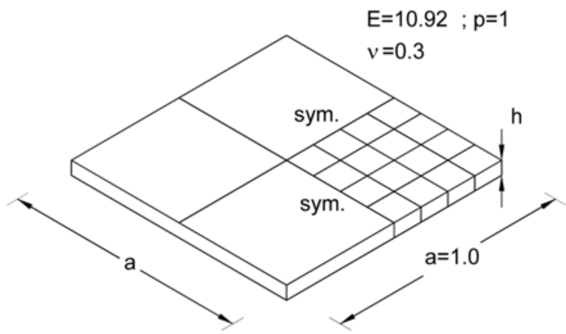

Fig. 6 A simply supported square plate with uniform loading

Table 5 Normalized central deflections for simply supported square plate

	h = 1		h = 0.1	
Element	2 × 2 mesh	4 × 4 mesh	2 × 2 mesh	4 × 4 mesh
Ibrahimbegovic and Wilson (1991)	0.959	0.986	0.583	0.806
Yunus *et al.* (1991)	1.033	1.058	0.981	1.005
Sze *et al.* (1996)	1.005	0.986	0.793	0.999
HBHEX8R (This study)	1.027	1.012	0.983	1.003

4.6 Example 6: Twisted beam

Fig. 7 depicts the 90° twisted beam. As all the elements warp, this problem constitutes a good test for membrane locking.

The end deflections are tabulated in Table 6 for two different mesh configurations.

The theoretical value is extracted from Mac-Neal and Harder (1985). Results showed that the behaviour of the present element is satisfactory and converges to the reference value.

To check the deterioration in element accuracy for different h/L values, normalized displacement parameter (wEh^3/pL^2) is obtained and given in Table 7.

The behaviour of the element, in case of small h/L values, deviates but is still in acceptable limits.

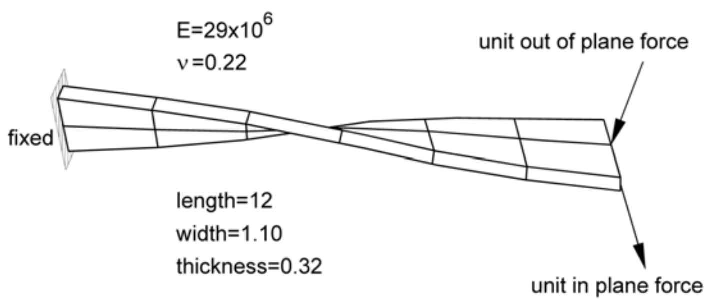

Fig. 7 Twisted beam

Table 6 End deflections of the twisted beam

	In plane		Out of plane	
	1 × 6	2 × 12	1 × 6	2 × 12
Pian and Tong (1986)	---	0.005429	---	0.001740
Yunus *et al.* (1991)	---	0.005429	---	0.001752
Sze *et al.* (1996)	---	0.005429	---	0.001752
Sze and Lo (1999)	0.005436	---	0.001753	---
Sze and Yao (2000)	0.005413	0.005429	0.001679	0.001736
HBHEX8R (This study)	0.005433	0.005427	0.001702	0.001753
Theoretical	0.005424		0.001754	

Table 7 Normalized displacement parameter ($w_{max}Eh^3/pL^4$) at the centre of uniformly loaded simply supported square plate

h/L	0.0001	0.005	0.015	0.03
In plane	0.9670	0.9745	0.9808	1.0028
Out of plane	1.0753	1.0739	1.0482	0.9579

4.7 Example 7: Hemispherical shell

A hemispherical shell with a 18° cut out is loaded by alternating point loads along *x*- and *y*-axis. Owing to symmetry, a quarter of the shell is modelled as shown in Fig. 8.

The computed deflections at the point of and the direction of loading are given in Table 8.

The reference value is extracted from Mac-Neal and Harder (1985). Results showed that the behaviour of the present element is satisfactory, converges to the reference value and is generally superior to the accuracies obtained by other elements.

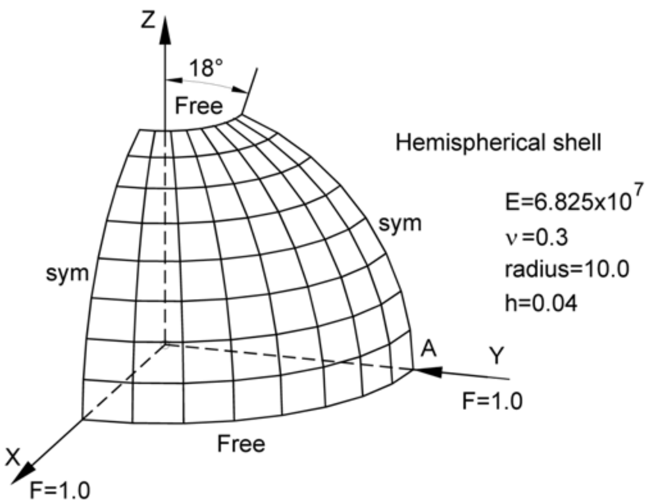

Fig. 8 Hemispherical shell

Table 8 Deflection for hemispherical shell problem

	Mesh			
	4 × 4	8 × 8	12 × 12	16 × 16
Pian and Tong (1984)	0.0038	0.0697	0.0899	---
Sze and Ghali (1993)	0.0987	0.0946	0.0938	---
Ooi *et al.* (2004)	0.0014	0.0575	---	0.0886
HBHEX8R (This study)	0.0991	0.0948	0.0943	0.0939
Reference	0.0940			

4.8 Example 8: Natural frequencies of a cantilever beam

The free vibration of a 10 × 0.1 × 0.1 cantilever beam is considered. The cantilever beam has been modelled with ten elements along the length and one across the cross section. All the degrees of freedom at the fixed end are restrained. The geometric and material characteristics are given in Fig. 9.

The first few flexural, axial and torsional frequencies are listed in Table 9.

The theoretical values shown in Table 9 have been computed using classical formulae available in literature (e.g., Timoshenko *et al.* 1974) which do not take into account the kinetic energy due to lateral motion induced by ν, and hence are meant for reference purposes only. It is seen that the predicted and computed values are in close agreement.

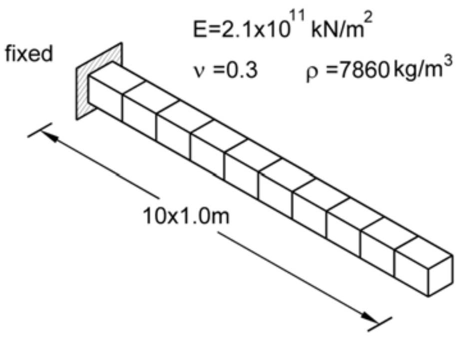

Fig. 9 Cantilever beam

Table 9 Natural frequencies (Hz) of cantilever beam

	Theory	Rajendran and Prathap (1999)	ANSYS SOLID45	HBHEX8R (This study)
Flexural	0.835	0.839	0.841	0.838
	5.231	5.383	5.397	5.257
	14.64	15.79	15.85	14.96
	28.66	33.36	33.51	30.76
Axial	129.2	130.3	130.4	130.09
	387.7	395.0	395.17	394.78
Torsional	80.14	80.19	80.22	80.18
	240.4	242.6	242.7	242.8

4.9 Example 9: Natural frequencies of a clamped square plate

The problem considered is a square plate with clamped edges. The geometric and material characteristics are given in Fig. 10. The plate is modelled with 8×8 meshes with one element

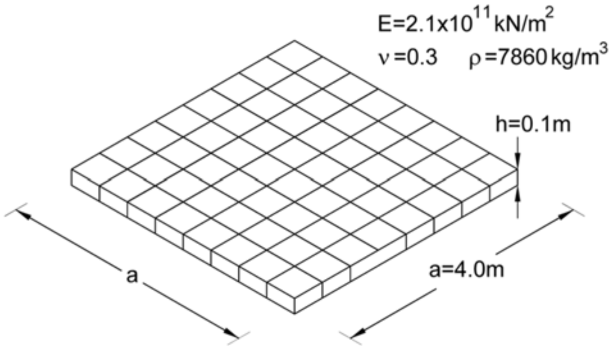

Fig. 10 Square plate with clamped edges

Table 10 Natural frequency coefficients for fully clamped square plate

Mode	Leissa (1969)	Rajendran and Prathap (1999)	Sze and Yao (2000)	Darılmaz (2005)	HBHEX8R (This study)
1	5.999	6.187	6.113	5.975	6.093
2,3	8.567	---	9.037	8.525	8.971
4	10.40	---	10.96	10.32	10.57
5,6	11.50	---	12.95	11.44	12.11

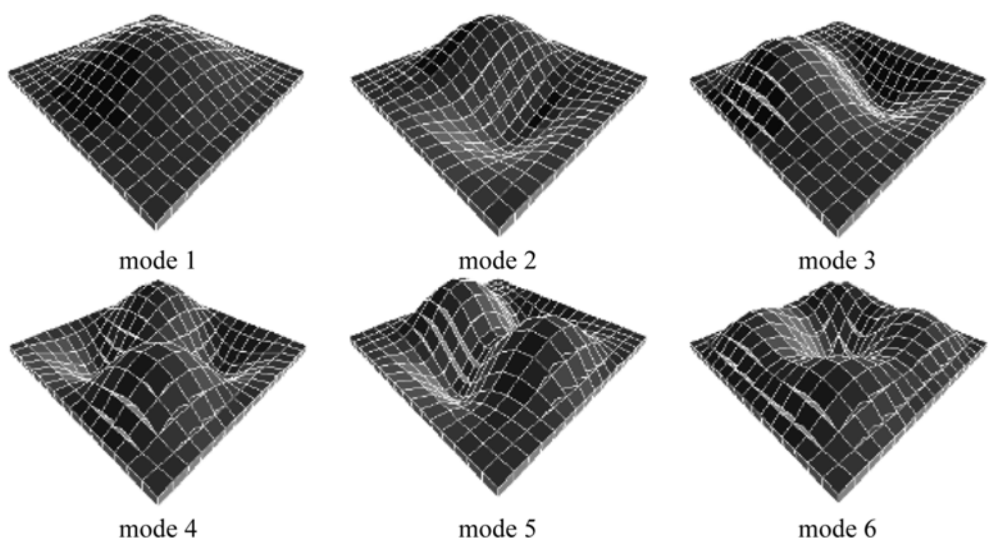

Fig. 11 First six modes of the square plate clamped on four edges

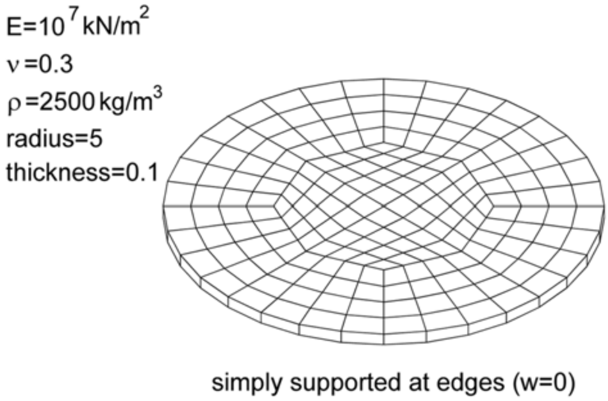

Fig. 12 Mesh configuration of the circular plate

through the depth.

Table 10 lists the predicted natural frequency coefficients, λ, defined by $\lambda^2 = 2\pi a^2\sqrt{\frac{\rho h}{D}}$ and the first six mode shapes of the plate are depicted in Fig. 11.

Results showed that the behaviour of the present element is satisfactory and results are in a good agreement with other solutions.

4.10 Example 10: Natural frequencies of a circular plate

A circular plate with a simply supported (w = 0 at edges) boundary condition is considered. The radius is chosen as R = 5 m and the material properties are Elasticity modulus $E = 10 \times 10^6$ kN/m^2, Poisson's ratio ν = 0.3, ρ = 2500 kg/m^3. This problem is interesting owing to the arbitrarily distorted mesh.

Nondimensionalized frequencies, $\omega r^2\sqrt{\rho h/D}$, where r is the radius, are computed for such a circular plate. In Table 11, the first six nondimensionalized frequencies are shown and compared with other solutions. Obviously, good agreement has been obtained for the thin cases.

The first six mode shapes of the circular plate are depicted in Fig. 13.

Table 11 Nondimensionalized frequencies $\omega r^2\sqrt{\rho h/D}$ for a simply supported circular plate

Mode number	HBHEX8R (This study)	HQP4 Darılmaz (2005)	Thin plate solution Leissa and Narita (1980)
1	5.061	4.799	4.9352
2	14.352	12.898	13.8982
3	14.352	12.898	13.8982
4	26.784	22.304	25.6133
5	26.813	22.352	25.6133
6	31.326	25.664	29.72

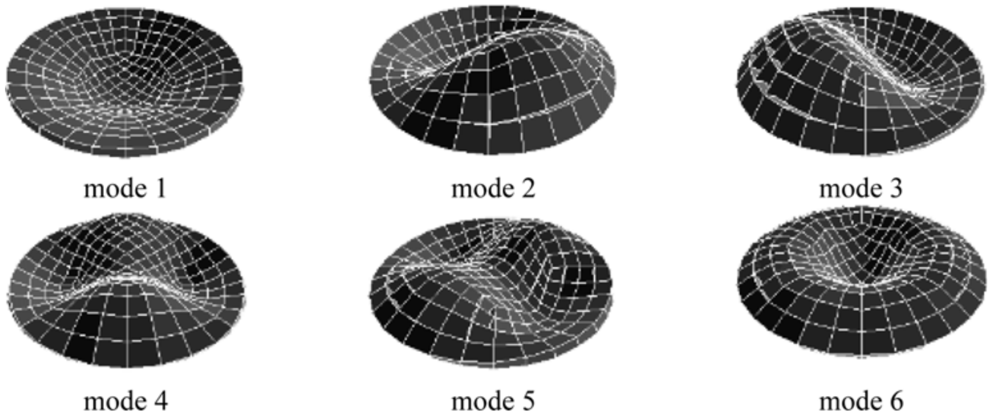

Fig. 13 First six modes of the circular plate

4.11 Example 11: Natural frequencies of a folded plate structure

The folded plate structure investigated in this example is illustrated in Fig. 14. The dimensions of the structure are based on units of L = 10 m, the width of 10 m and thickness 0.5 m. The material properties used are $E = 2.1 \times 10^6$, $\nu = 0.3$ and $\rho = 2500$ kg/m^3.

The first six circular frequencies of the system are determined and given in Table 12.

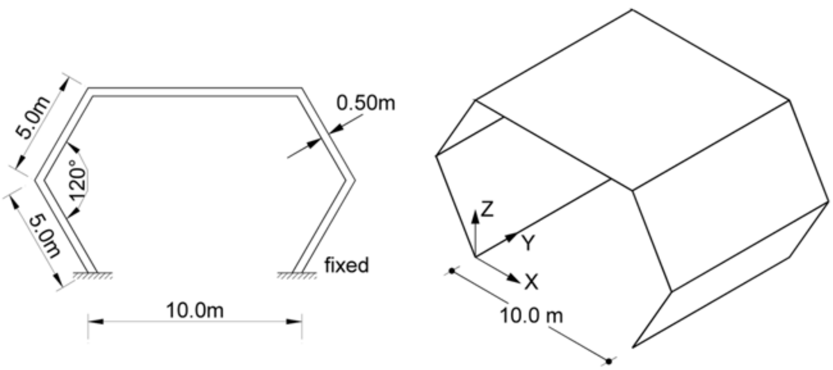

Fig. 14 Fixed supported folded plate structure

Table 12 Frequencies (f) for the folded plate structure

Mode number	ANSYS (SOLID45) (640 Elements)	HBHEX8R (160 Elements)
1	0.834	0.833
2	1.796	1.790
3	1.849	1.831
4	3.551	3.529
5	3.677	3.648
6	5.247	5.213

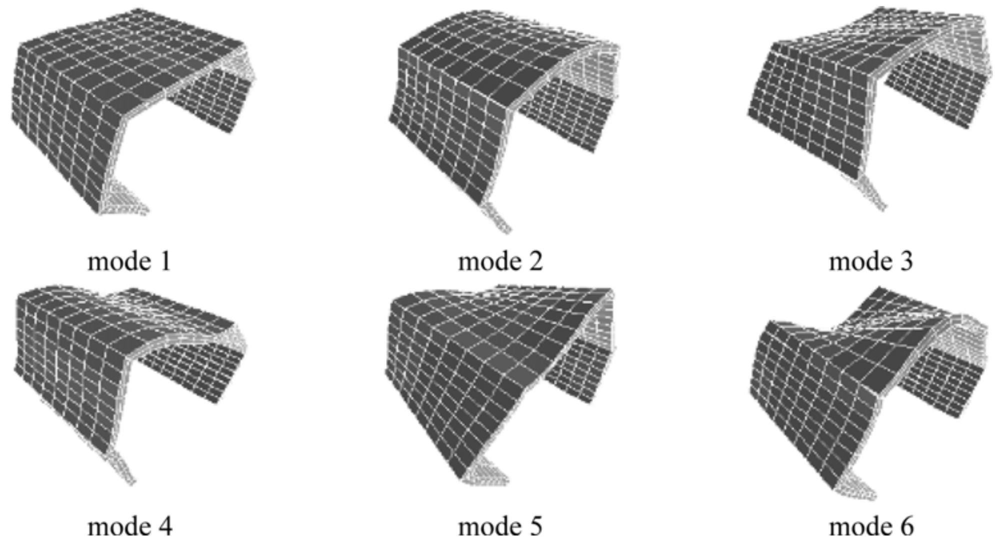

Fig. 15 First six modes of the folded plate structure

In Fig. 15 the first six mode shapes of the folded plate are depicted.

Results obtained are in a good agreement with ANSYS SOLID45 element solutions. Even with coarser mesh, the present element solutions have a good accuracy.

5. Conclusions

The main goal of this study is to investigate the performance of the HBHEX8R element in static and free vibration analysis. A number of numerical problems are utilized to assess the performance of the present element. Numerical comparisons show that the present element yields comparatively satisfactory and accurate results. The behaviour in case of element distortion deviates but is still in general qualitatively comparable. The element is currently used in linear analysis. Further research is underway to investigate the validity of the element in the nonlinear environment.

Acknowledgements

The author gratefully acknowledges the excellent support and encouragement provided by Professor Dr. Nahit Kumbasar.

References

ANSYS, Swanson Analysis Systems, Swanson J., ANSYS 5.4. USA.

Cao, Y.P., Hu, N., Lu, J., Fukunaga, H. and Yao, Z.H. (2002), "A 3D brick element based on Hu-Washizu variational principle for mesh distortion", *Int. J. Num. Meth. Eng.*, **53**, 2529-2548.

Chandra, S. and Prathap, G. (1989), "A field-consistent formulation for the 8-noded solid finite element", *Comp. Struct.*, **33**, 345-355.
Chen, Y.I. and Wu, G.Y. (2004), "A mixed 8-node hexahedral element based on the Hu-Washizu principle and the field extrapolation technique", *Struct. Eng. Mech.*, **17**(1), 113-140.
Chen, W.J. and Cheung, Y.K. (1992), "Three-dimensional 8-node and 20-node refined hybrid isoparametric elements", *Int. J. Num. Meth. Eng.*, **35**, 1871-1889.
Choi, C.K. and Chung, K.Y. (1996), "Three dimensional non-conforming 8-node solid elements with rotational degrees of freedom", *Struct. Eng. Mech.*, **4**(5), 569-586.
Choi, C.K., Chung, K.Y. and Lee, E.J. (2001), "Mixed formulated 13-node hexahedral elements with rotational degrees of freedom: MR-H13 elements", *Struct. Eng. Mech.*, **11**(1), 105-122.
Choi, C.K. and Lee, N.H. (1993), "Three dimensional transition solid elements for adaptive mesh gradation", *Struct. Eng. Mech.*, **1**(1), 61-74.
Darılmaz, K. (2005), "An assumed-stress finite element for static and free vibration analysis of Reissner-Mindlin plates", *Struct. Eng. Mech.*, **19**(2), 199-215.
Feng, W., Hoa, S.V. and Huang, Q. (1997), "Classification of stress modes in assumed stress fields of hybrid finite elements", *Int. J. Num. Meth. Eng.*, **40**, 4313-4339.
Ibrahimbegovic, A. and Wilson, E.L. (1991), "Thick shell and solid finite elements with independent rotation fields", *Int. J. Num. Meth. Eng.*, **31**, 1393-1414.
MacNeal, R.H. and Harder, R.L. (1985), "A proposed standard set of problems to test finite element accuracy", *Finite Elem. Anal. Des.*, **1**, 3-20.
MacNeal, R.H. and Harder, R.L. (1988), "A refined four-noded membrane element with rotational degrees of freedom", *Comp. Struct.*, **28**, 75-84.
Leissa, A.W. (1969), *Vibration of Plates*, Scientific and Technical Information Division, NASA, Washington, DC.
Leissa, A.W. and Narita, Y. (1980), "Natural frequencies of simply supported circular plates", *J. Sound Vib.*, **70**(2), 221-229.
Ooi, E.T., Rajendran, S. and Yeo, J.H. (2004), "A 20-node hexahedron element with enhanced distortion tolerance", *Int. J. Numer. Meth. Engng.*, **60**(15), 2501-2530.
Pian, T.H.H. (1964), "Derivation of element stiffness matrices by assumed stress distributions", *AIAA J.*, **2**, 1333-1336.
Pian, T.H.H. and Chen, D.P. (1983), "On the suppression of zero energy deformation modes", *Int. J. Num. Meth. Eng.*, **19**, 1741-1752.
Pian, T.H.H. and Sumihara, K. (1984), "Rational approach for assumed stress finite elements", *Int. J. Numer. Meth. Engng.*, **20**, 1685-1695.
Pian, T.H.H. and Tong, P. (1986), "Relations between incompatible model and hybrid stress model", *Int. J. Num. Meth. Eng.*, **22**, 173-181.
Punch, E.F. and Atluri, S.N. (1984), "Development and testing of stable, isoparametric curvilinear 2 and 3-D hybrid stress elements", *Comput. Meth. Appl. Mech. Eng.*, **47**, 331-356.
Rajendran, S. and Prathap, G. (1999), "Eight-node field-consistent hexahedron element in dynamic problems", *Struct. Eng. Mech.*, **8**(1), 19-26.
Sze, K.Y. and Ghali, A. (1993), "Hybrid hexahedral element for solids, plates, shells and beams by selective scaling", *Int. J. Num. Meth. Eng.*, **36**, 1519-1540.
Sze, K.Y. and Lo, S.H. (1999), "A 12-node hybrid stress brick element for beam/column analysis", *Eng. Comp.*, **16**(6-7), 752-766.
Sze, K.Y. and Pan, Y.S. (2000), "Hybrid stress tetrahedral elements with Allman's rotational D.O.F.s", *Int. J. Num. Meth. Eng.*, **48**, 1055-1070.
Sze, K.Y., Soh, A.K. and Sim, Y.S. (1996), "Solid elements with rotational DOFs by explicit hybrid stabilization", *Int. J. Num. Meth. Eng.*, **39**, 2987-3005.
Sze, K.Y. and Yao, L.Q. (2000), "A hybrid stress ANS solid-shell element and its generalization for smart structure modelling. Part I-solid-shell element formulation", *Int. J. Numer. Meth. Engng.*, **48**, 545-564.
Timoshenko, S. and Goodier, J.N. (1951), *Theory of Elasticity*, Mc-Graw Hill, New York.
Timoshenko, S., Young, D.H. and Weaver Jr. W. (1974), *Vibration Problems in Engineering*, 4th. ed., John Wiley & Sons, New York.

Yeo, S.T. and Lee, B.C. (1997), "New stress assumption for hybrid stress elements and refined four-node plane and eight-node brick elements", *Int. J. Num. Meth. Eng.*, **40**, 2933-2952.

Yunus, S.M., Saigal, S. and Cook, R.D. (1989), "On improved hybrid finite elements with rotational degrees of freedom", *Int. J. Num. Meth. Eng.*, **28**, 785-800.

Yunus, S.M., Pawlak, T.P. and Cook, R.D. (1991), "Solid elements with rotational degrees of freedom: Part 1-hexahedral elements", *Int. J. Num. Meth. Eng.*, **31**, 573-592.

Notation

a	: length of the plate edge
h	: thickness
E	: modulus of elasticity
f	: frequency
D	: flexural rigidity of the plate
V	: volume of an element
γ	: dimensionless constant
λ	: frequency parameter
ν	: Poisson ratio
ρ	: mass per unit volume
ω	: angular frequency
$\bar{u}, \bar{v}$	: in plane translations in the face coordinate system
$\bar{x}, \bar{y}$	: face system coordinate
$[D]$	: differential operator matrix
$[G]$	: nodal forces corresponding to assumed stress field
$[N]$	: shape functions
$[P]$	: interpolation matrix for stress
$[R]$	: inertia matrix
$[S]$	: material compliance matrix
$[T]$	: transformation matrix
$\{q\}, \{\dot{q}\}$	: displacement and velocity components
$\{\bar{q}\}$	: face system nodal unknowns
$\{u\}$	: displacements
$\{\beta\}$	: stress parameters
$\{\sigma\}, \{\tilde{\sigma}\}$	: stress
$\{\varepsilon\}$	: strain
$[\Phi]$	: relative rotation in terms of face system unknowns